physica status solidi rrl

www.pss-rapid.com

Controlled Current Transport in Pt/Nb:$SrTiO_3$ Junctions via Insertion of Uniform Thin Layers of TaO_x

Atsushi Tsurumaki-Fukuchi, Yusuke Tsuta, Masashi Arita, and Yasuo Takahashi*

Systematic control of electronic transport is demonstrated for Pt/Nb-doped $SrTiO_3$ (Nb:STO) junctions based on interface engineering with uniform thin layers of TaO_x. By inserting TaO_x layers fabricated via sputter deposition with different O_2–Ar ratios (r_{O2}), the current–voltage characteristics and behavior of resistive switching can be well controlled in Pt/Nb:STO junctions. Reduction of the Schottky barrier is also demonstrated via the insertion, and formation of an ideal ohmic contact with a low contact resistance of $<3\,\Omega$ is achieved for $r_{O2} = 0\%$. Structural and chemical characterizations show that the resistivity of the TaO_x layers depends significantly on r_{O2} while maintaining a uniform structure independent of the resistivity. This indicates that the insertion of both insulating and metallic interface layers is possible by sputtering TaO_x with no need for epitaxial growth, suggesting TaO_x's potential as an interface-layer material. Even with very thin layers (1.0 nm) of TaO_x the interfacial properties can be controlled to enhance both ohmic contact formation and resistive switching. These results demonstrate an easy and reliable way to control the characteristics of Pt/Nb:STO junctions and present new insights for their memory and semiconductor device applications.

Schottky barrier engineering in metal/oxide junctions has been considered an important issue of recent oxide electronics. At metal/oxide semiconductor junctions, the Schottky barrier can be altered by external voltages through transport of trapped charges and/or oxygen ion migration. These phenomena are known to cause "interface-type" resistive switching,[1–11] which has been actively investigated for its applications in memory and neuromorphic devices owing to its intrinsic multi-level/analog switching capability.[1,2,6,7,9,10] Pt/Nb-doped $SrTiO_3$ (Nb:STO) junctions are known to show clear interfacial resistive switching under reverse bias[2,4–8] with relatively high performances.[2] However, the controllability and reproducibility of the resistive switching of Pt/Nb:STO is poor because they are highly sensitive to fabrication conditions.[2,7] Recent studies suggest that the variations of Pt/Nb:STO junction characteristics may be reduced by inserting an insulating interface layer.[7,8] However, the ability to control the junction characteristics via interface engineering is generally limited because of extrinsic influences from the structural inhomogeneity of the interface layers.[8] Thus, an interface-layer material with a high structural uniformity needs to be developed for applications of Pt/Nb:STO Schottky junctions.

Pt/Nb:STO junctions also have another important requirement with regard to the Schottky barrier, namely reduction of the barrier height. Reduction of the interfacial resistance is considered a crucial step for many electronic applications of STO,[12,13] because STO's wide band gap (3.3 eV) easily forms a high (>1.0 eV) Schottky barrier with an electrode[14,15] causing a high contact resistance. In metal/oxide junctions, interface engineering has also been demonstrated to be effective at reducing the barrier height.[16–20] In $SrRuO_3$/Nb:STO epitaxial junctions, formation of a good ohmic contact has been achieved by inserting a thin epitaxial $LaAlO_3$ interfacial layer.[16,17,20] For Pt, which is the most widely used electrode for oxides, however, no appropriate interface-layer material has been proposed for ohmic contact formation. The difficulty of finding a suitable interface material may originate from the large difference in the crystal structures of Pt and STO, which makes the formation of a coherent interface layer difficult.

In this study, we investigated the possibility of barrier height engineering and the control of resistive switching in Pt/Nb:STO junctions based on interface engineering with TaO_x layers. Recently, some studies have reported the occurrence of high structural uniformity for crystalline and amorphous TaO_x,[21,22] and we have thus tried to exploit those structural advantages for fabricating junctions. In Pt/TaO_x/Nb:STO junctions with engineered interfaces we successfully demonstrated both formation of an ideal ohmic contact and an enhancement of the resistive switching by controlling the O_2–Ar ratio during the sputter deposition of TaO_x. The demonstrated high controllability of the junction characteristics may provide a new basis for the wide-scale application of metal/oxide junctions.

Pt(50 nm)/TaO_x(1–10 nm)/Nb:STO(001) junctions with a dimension of 100 μm^2 were fabricated by radio frequency sputtering of Pt and TaO_x layers onto single-crystalline Nb:STO (0.05 wt.% Nb) substrates through a shadow mask. Sputtering was conducted at room temperature in an O_2 + Ar atmosphere (total pressure of 1.0 Pa). The oxygen concentrations in the

Dr. A. Tsurumaki-Fukuchi, Y. Tsuta, Prof. M. Arita, Prof. Y. Takahashi
Graduate School of Information Science and Technology
Hokkaido University
Sapporo, Hokkaido 060-0814, Japan
E-mail: a.fukuchi@ist.hokudai.ac.jp

The ORCID identification number(s) for the author(s) of this article can be found under https://doi.org/10.1002/pssr.201900136.

DOI: 10.1002/pssr.201900136

sputtering atmosphere (r_{O2}: $O_2/(O_2 + Ar)$) were varied from 0 to 50% by controlling the mass-flow ratio of the inlet O_2 and Ar. A sputtering power of 100 W and target-to-substrate distance of 80 mm were used for the depositions. The TaO_x layers were characterized via X-ray photoelectron spectroscopy (XPS; ESCA-3400, Shimadzu, Japan) and atomic force microscopy (Nanocute, Hitachi High-Technologies Co., Japan). The Pt/TaO_x/Nb:STO junctions' current–voltage (I–V) and capacitance–voltage (C–V) characteristics were measured using a B1500 semiconductor parameter analyzer (Keysight Co, USA) and 4274A multi-frequency LCR meter (Yokogawa Hewlett Packard Ltd., Japan), respectively. I–V and C–V measurements were conducted at room temperature with grounded Nb:STO substrates; the measurement frequency for the C–V measurements was 100 kHz.

We observed that the transport properties of Pt/TaO_x/Nb:STO junctions systematically changed depending on the r_{O2} in the TaO_x depositions. **Figure 1**(a) shows the r_{O2} dependence of the deposition rate of the TaO_x layers as determined via thicknesses measurements. The deposition rate peaked initially, before dropping to a lower level at higher r_{O2} and plateauing there. This behavior is typical for reactive sputtering in a hysteresis mode,[23,24] which is defined by the dependence of the deposition rate on the history of the reactive gas inlet flow. For the TaO_x depositions we observed hysteresis behavior in the deposition rate for r_{O2} values of 1–30%. We thus assumed that the hysteresis region is present in this range for our TaO_x layers, and the reduction of the deposition rate at $r_{O2} = 30$–40% is a result of a transition into reactive mode.[23,24] It should be noted that all depositions in this study were performed by setting the r_{O2} values with O_2 flow was decreased from $r_{O2} > 50\%$. The TaO_x layers' in-plane resistivity showed a rapid increase at $r_{O2} = 9\%$ (Figure 1(b)), and further increased above the measurement limit (1 kΩcm) for $r_{O2} \geq 10\%$. This suggests that the stoichiometry borderline[23] of TaO_x between $x < 2.5$ and $x = 2.5$ is present at an r_{O2} of around 9% (Figure 1(a) and Figure S1, Supporting Information). We also observed that the TaO_x layers maintained a high structural uniformity across the entire range of $r_{O2} = 0$–50%, although there was a large change in the resistivity from metallic to insulating. Figure 1(c) shows that both the TaO_x layers at $r_{O2} = 0$ and 50% are free from grain boundaries and have a very smooth surface (root mean square roughness = 0.1 nm).

By inserting the uniform TaO_x layers into Pt/Nb:STO structures, we achieved systematic control of the junction properties. As shown in **Figure 2**(a), the I–V characteristics of Pt/TaO_x(10 nm)/Nb:STO junctions drastically changed from ohmic to rectifying when r_{O2} was increased. We also observed clear resistive switching behavior in the junctions with $r_{O2} \geq 9\%$ in the reverse bias regime (Figure S1, Supporting Information for details). For $r_{O2} \leq 7\%$, the junction resistance was significantly reduced compared with Pt/Nb:STO junctions, and the I–V characteristics became linear. A good ohmic contact with a low resistance of $<3\,\Omega$ was formed at $r_{O2} = 0\%$. By inserting TaO_x layers with $r_{O2} \geq 9\%$ the switching ratios (estimated from the differences between the reverse bias currents' upper and lower branches) were increased compared with those of non-engineered Pt/Nb:STO(0.05 wt.%) junctions (Figure 2(a)), and control over the switching ratio by varying r_{O2} was demonstrated. The increase in the switching ratio was finally saturated for $r_{O2} \geq 40\%$ (Figure S1(a), Supporting Information). We found

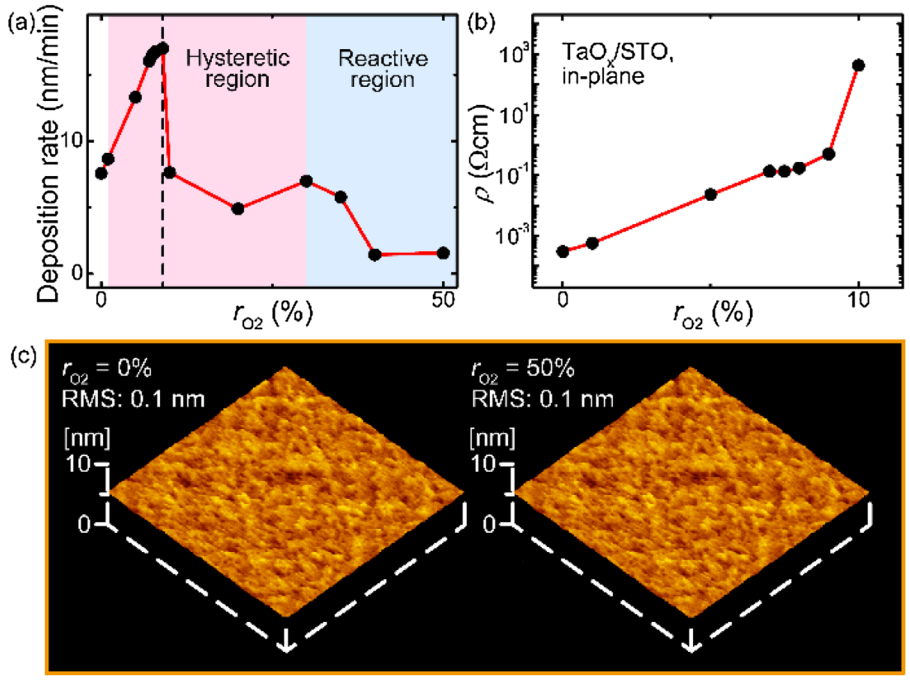

Figure 1. a) r_{O2} dependence of the deposition rate of the TaO_x layers. The dashed line represents the expected stoichiometry borderline between $x < 2.5$ and $x = 2.5$. b) r_{O2} dependence of the TaO_x layers' in-plane resistivity measured on non-doped STO substrates. c) Atomic force microscopy images of TaO_x(10 nm)/Nb:STO samples with an r_{O2} of 0% (left panel) and 50% (right panel). The scanned area was $3.0 \times 3.0\,\mu m^2$.

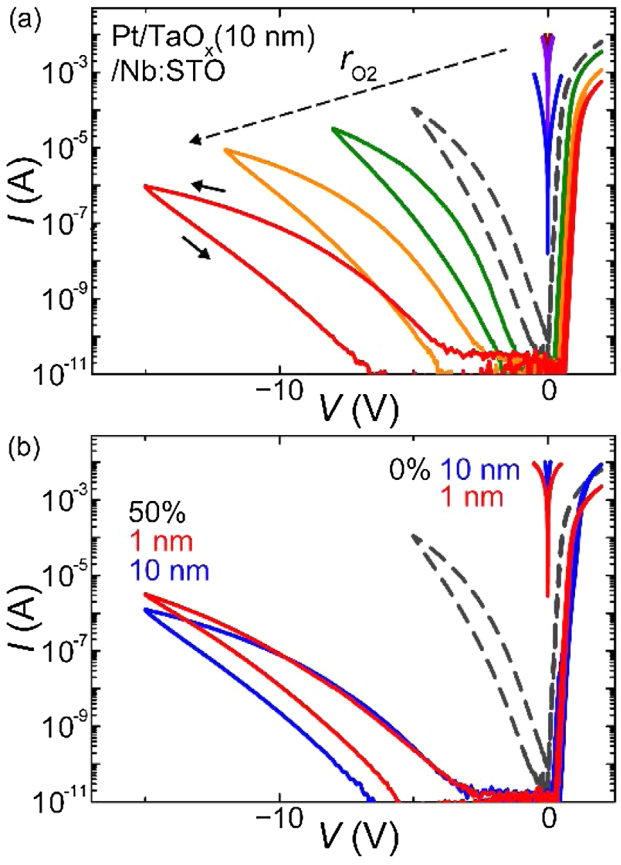

Figure 2. a) *I–V* characteristics of Pt/TaO_x(10 nm)/Nb:STO junctions with $r_{O2} = 0$, 5, 7, 30, 35, and 40%. The dashed curves represent the *I–V* characteristics measured for a non-engineered Pt/Nb:STO junction. b) TaO_x-thickness dependence of the *I–V* characteristics for Pt/TaO_x/Nb:STO junctions with $r_{O2} = 0$ and 50%.

that the formation of an ohmic contact was possible even with a very thin (1-nm-thick) TaO_x layer at $r_{O2} = 0\%$ (Figure 2(b)). The effective thickness of 1 nm is comparable to that of the epitaxial interface layers reported in metal/oxide heteroepitaxial junctions for ohmic contact formation.[16,17,20] This very thin thickness may come from high interfacial coverage for Nb:STO owing to the structural uniformity of TaO_x (Figure 1(c)). Resistive switching was also enhanced with a 1-nm-thick TaO_x layer at $r_{O2} = 50\%$ (Figure 2(b)). This also suggests that the changes in the resistive switching behaviors are derived from an interfacial effect at the TaO_x/Nb:STO interface rather than from the TaO_x layers' bulk properties.

XPS measurements showed that the TaO_x layers on the Nb:STO substrates included a significant amount of Ta^{5+} (Ta_2O_5) phase even at $r_{O2} = 0\%$ (**Figure 3**(a)). The Ta_2O_5 phase is considered to be a product of interface reactions with Nb:STO[22] and atmospheric oxidation via the surface.[25] We observed that the amount of Ta^{0+}, Ta^{2+}, and Ta^{4+} phases decreased as r_{O2} was increased, and only small amounts of Ta^{2+} and Ta^{4+} remained at $r_{O2} = 7.5\%$. Only Ta^{5+} peaks could be observed above the deposition rate maximum at $r_{O2} = 9\%$. As shown in Figure 3(a), almost no change in the spectra were observed for r_{O2} of 20 and 50%. This shows that the oxidation states of TaO_x are similar in the r_{O2} range of 10–50% and that x is ≈2.5.

The junction capacitances of Pt/TaO_x(10 nm)/Nb:STO were significantly reduced compared with those of Pt/Nb:STO junctions (≈210 pF at 0 V compared with ≈450 pF at 0 V), but showed no clear dependence on r_{O2} for r_{O2} values of 10–50% (Figure 3(b)). With regard to the devices' capacitances, only small differences (≈several percent) were observed between the high resistance state (HRS, after negative voltages) and low resistance state (LRS, after positive voltages), in agreement with previous reports.[6,7] The capacitance independence of r_{O2} suggests that the dielectric constants, carrier concentrations, and built-in potentials (determined form the abscissa intercepts in C^{-2}–V plots)[26,27] of the Pt/TaO_x/Nb:STO junctions do not have a systematic relationship with r_{O2} in the r_{O2} range of 10–50%. This is consistent with the XPS results, which show similar oxidation states of TaO_x for the TaO_x layers fabricated in this r_{O2} range.

From the forward bias *I–V* characteristics (Figure 2 and Figure S1, Supporting Information), we estimated the Schottky barrier heights (ϕ_B) of the Pt/TaO_x/Nb:STO junctions using the thermionic emission model. The ϕ_B values show a clear dependence on r_{O2} in the 10–50% region (Figure 3(c)), whereas the *C–V* measurements suggest that the built-in potentials are independent of r_{O2} in this range. The deviation between the values of ϕ_B determined from the *I–V* and *C–V* characteristics is typical of Pt/Nb:STO junctions and has been attributed to the formation of local low-resistance regions at the junction interfaces.[4–6] From this perspective, the *C–V* characteristics (Figure 3(b)) can be treated as the areal sums of the overall junction capacitances, while the *I–V* characteristics (Figure 2) can be treated as predominantly caused by large current flows in local regions with lower ϕ_B. We observed that the ϕ_B (for the local low-resistance regions) had a clear inverse relationship with the ideality factor n (Figure 3(c)). In addition, ϕ_B and n showed a correlation with TaO_x's deposition rate (Figure 1(a)): ϕ_B and n increased and decreased, respectively, as the deposition rate decreased.

The migration of oxygen defects cannot be excluded from the list of possible origins of the hysteretic behaviors of the *I–V* characteristics; however, this mechanism is unlikely to actually be the cause because our junctions showed larger switching at higher oxidation states of TaO_x. In contrast, our results suggest that the density of interfacial charges may be systematically affected by r_{O2} in the Pt/TaO_x/Nb:STO junctions. In a metal/semiconductor Schottky junction with a thick interface layer, n is expressed as

$$n = 1 + \frac{\delta}{\varepsilon_i}\left(\frac{\varepsilon_s}{W} + qD_{sb}\right) \quad (1)$$

where δ and W are the thicknesses of the interface and depletion layers, respectively; ε_i and ε_s are the dielectric constants; q is the elementary charge; and D_{sb} is the density of interfacial states in equilibrium with the semiconductor.[26,28] The XPS results suggest that in our junctions the ε_i of TaO_x is constant for $r_{O2} = 10$–50%, while the *C–V* measurements suggest that ε_s and W have no systematic dependence on r_{O2}. The decrease in n with increased r_{O2} (Figure 3(c)) can thus be assumed to be the result of a decrease in the density of the interface states at the TaO_x/Nb:

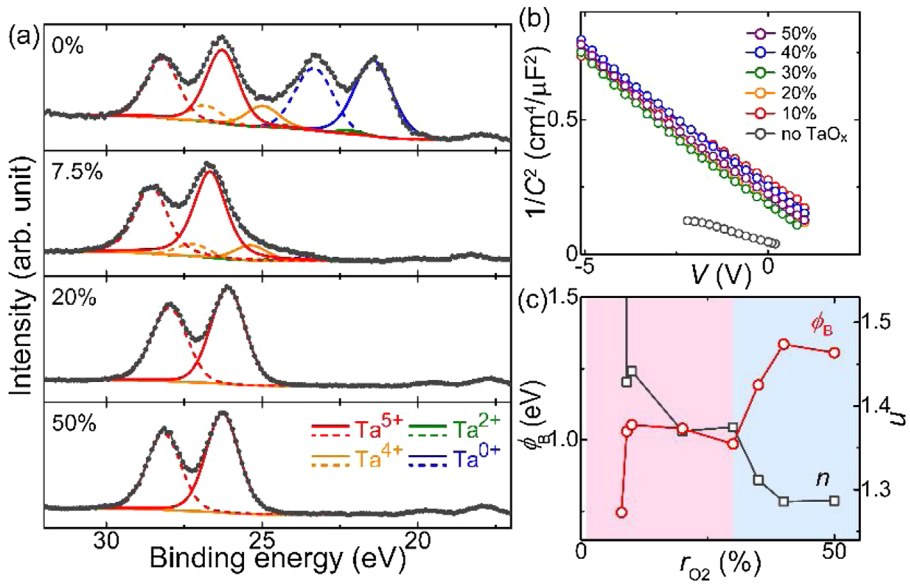

Figure 3. a) XPS spectra of TaO_x(10 nm)/Nb:STO layers with $r_{O2} = 0$–50% in the vicinity of the Ta-4f peaks. b) C^{-2}–V plots for Pt/TaO_x(10 nm)/Nb:STO junctions with $r_{O2} = 10$–50% in the HRS. c) r_{O2} dependences of the ϕ_B and n of Pt/TaO_x(10 nm)/Nb:STO junctions determined from the I–V characteristics under forward bias. The pink and light blue background areas represent the hysteresis and reactive region of the deposition rate, respectively.

STO interface (D_{sb}). This assumption seems reasonable because a slower TaO_x deposition rate at a higher r_{O2} will form a lower density of interface defects.

On the basis of the changes in D_{sb}, we propose that they may be the origin of the r_{O2} dependence of the hysteretic I–V characteristics. In Pt/Nb:STO junctions (**Figure 4**(a)) ϕ_B is known to be reduced from 1.4 eV at the Schottky limit to ≈1.1 eV by Fermi-level pinning[14,15] through charge transfer from interface states on Nb:STO to Pt. In the Pt/TaO_x/Nb:STO junctions with $r_{O2} < 9\%$, the depletion width will be further reduced by electron doping from oxygen vacancies formed through interfacial scavenging reactions with TaO_x[22] (Figure 4(b)). In $r_{O2} > 9\%$, where insulating Ta_2O_5 is formed, the vacancy doping effect will be significantly reduced, and a high barrier to Nb:STO will form. The lower reverse bias currents in $r_{O2} > 9\%$ (Figure 2(a) and Figure S1(a), Supporting Information) suggest that the ϕ_B is higher than in Pt/Nb:STO junctions, possibly caused by a reduced D_{sb} owing to the TaO_x layer insertion. When positive voltages are applied to the Pt/TaO_x/Nb:STO junctions (Figure 4(c)), the trapped interface charges will be locally discharged from Nb:STO to Pt and ϕ_B will be locally decreased, as previously reported for Nb:STO junctions.[3–6] By applying negative voltages to the junctions (Figure 4(d)), the discharged interface levels will be refilled, and the reduced barriers will return to a higher state.[4–6] We propose that the local alterations in φ_B are a possible origin of the resistive switching and that the enhancement caused by the TaO_x layer insertion can be attributed to the decrease in D_{sb}. Regarding the interfacial trapping/detrapping of electrons,[3–6] the energetic requirements for the charging and discharging should depend on D_{sb}. A lower D_{sb} at higher r_{O2} may thus cause a slower, non-transient recovery of the LRS and form a larger hysteresis loop in the reverse bias I–V characteristics, as observed in the junctions with an r_{O2} of ≥9%.

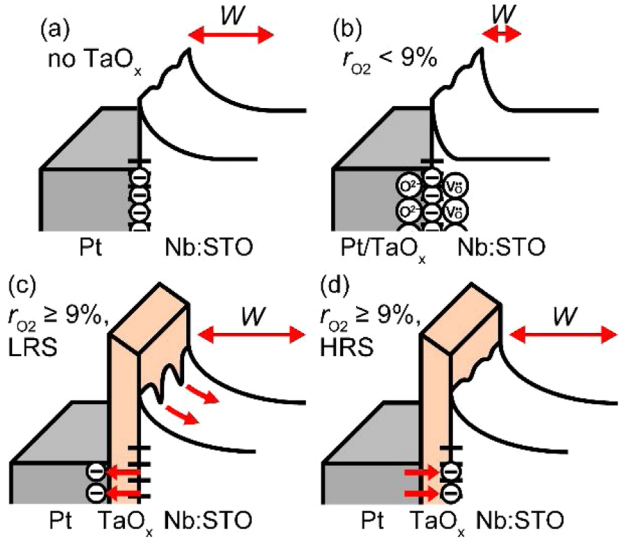

Figure 4. Schematic energy band diagrams of a (a) Pt/Nb:STO junction, and Pt/TaO_x/Nb:STO junction with r_{O2} of (b) <9%, (c) ≥9% in the LRS, and (d) ≥9% in the HRS. The short horizontal lines at Nb:STO interfaces represent the interface states.

In summary, control of the band alignment and interface resistive switching in Pt/Nb:STO junctions was demonstrated by interface engineering using TaO_x layers. Incorporating a single material (TaO_x) into this junction and varying r_{O2} during its deposition allowed both the formation of an ideal ohmic contact and significantly enhanced resistive switching. Our results suggest that the barrier height reduction was achieved through

oxygen scavenging of TaO_x and that the enhancement of the resistive switching can be attributed to a reduction in the density of interfacial trapped charges, which was directly achieved by the insertion of the TaO_x layer. These findings provide a convenient way of forming ohmic contacts at metal/oxide junctions and a way toward highly reliable interface resistive switching.

Supporting Information

Supporting Information is available from the Wiley Online Library or from the author.

Acknowledgments

Part of this work was financially supported under KAKENHI by the Japan Society for the Promotion of Science (JSPS) (Nos. 16K18073, 16H04339, and 15H01706). The authors acknowledge Nippon Sheet Glass Foundation for Materials Science and Engineering, the Scholar Project of the Toyota Physical and Chemical Research Institute, and the Hattori-Hokokai Foundation for their financial support of this work.

Conflict of Interest

The authors declare no conflict of interest.

Keywords

interface engineering, resistive switching, Schottky junctions, $SrTiO_3$, tantalum oxides

Received: March 7, 2019
Revised: April 1, 2019
Published online:

[1] A. Sawa, T. Fujii, M. Kawasaki, Y. Tokura, *Appl. Phys. Lett.* **2004**, *85*, 4073.
[2] H. Sim, H. Choi, D. Lee, M. Chang, D. Choi, Y. Son, E.-H. Lee, W. Kim, Y. Park, I.-K. Yoo, H. Hwang, in *IEEE International Electron Devices Meeting, IEDM Technical Digest,* Washington, DC, **2005**, 758.
[3] T. Fujii, M. Kawasaki, A. Sawa, Y. Kawazoe, H. Akoh, Y. Tokura, *Phys. Rev. B* **2007**, *75*, 165101.
[4] J. Li, N. Ohashi, H. Okushi, H. Haneda, *Phys. Rev. B* **2011**, *83*, 125317.
[5] E. Lee, M. Gwon, D.-W. Kim, H. Kim, *Appl. Phys. Lett.* **2011**, *98*, 132905.
[6] D. Kan, Y. Shimakawa, *Appl. Phys. Lett.* **2013**, *103*, 142910.
[7] E. Mikheev, B. D. Hoskins, D. B. Strukov, S. Stemmer, *Nat. Commun.* **2014**, *5*, 3990.
[8] E. Mikheev, J. Hwang, A. P. Kajdos, A. J. Hauser, S. Stemmer, *Sci. Rep.* **2015**, *5*, 11079.
[9] K. Baek, S. Park, J. Park, Y.-M. Kim, H. Hwang, S. H. Oh, *Nanoscale* **2017**, *9*, 582.
[10] S. Bagdzevicius, K. Maas, M. Boudard, M. Burriel, *J. Electroceramics* **2017**, *39*, 157.
[11] N. Du, N. Manjunath, Y. Li, S. Menzel, E. Linn, R. Waser, T. You, D. Bürger, I. Skorupa, D. Walczyk, C. Walczyk, O. G. Schmidt, H. Schmidt, *Phys. Rev. Appl.* **2018**, *10*, 054025.
[12] A. Ohtomo, H. Y. Hwang, *Nature* **2004**, *427*, 423.
[13] J. Son, P. Moetakef, B. Jalan, O. Bierwagen, N. J. Wright, R. Engel-Herbert, S. Stemmer, *Nat. Mater.* **2010**, *9*, 482.
[14] J. Robertson, C. W. Chen, *Appl. Phys. Lett.* **1999**, *74*, 1168.
[15] J. Robertson, *J. Vac. Sci. Tech. B* **2000**, *18*, 1785.
[16] T. Yajima, M. Minohara, C. Bell, H. Kumigashira, M. Oshima, H. Y. Hwang, Y. Hikita, *Nano Lett.* **2015**, *15*, 1622.
[17] T. Yajima, Y. Hikita, M. Minohara, C. Bell, J. A. Mundy, L. F. Kourkoutis, D. A. Muller, H. Kumigashira, M. Oshima, H. Y. Hwang, *Nat. Commun.* **2015**, *6*, 6759.
[18] T. Tachikawa, M. Minohara, Y. Hikita, C. Bell, H. Y. Hwang, *Adv. Mater.* **2015**, *27*, 7458.
[19] T. Tachikawa, H. Y. Hwang, Y. Hikita, *Appl. Phys. Lett.* **2017**, *111*, 091602.
[20] T. Yajima, M. Minohara, C. Bell, H. Y. Hwang, Y. Hikita, *Appl. Phys. Lett.* **2018**, *113*, 221603.
[21] Y. Guo, J. Robertson, *Appl. Phys. Lett.* **2014**, *104*, 112906.
[22] A. Tsurumaki-Fukuchi, R. Nakagawa, M. Arita, Y. Takahashi, *ACS Appl. Mater. Interfaces* **2018**, *10*, 5609.
[23] S. Schiller, G. Beister, W. Sieber, *Thin Solid Films* **1984**, *111*, 259.
[24] S. Berg, T. Nyberg, *Thin Solid Films* **2005**, *476*, 215.
[25] R. Schmiedl, V. Demuth, P. Lahnor, H. Godehardt, Y. Bodschwinna, C. Harder, L. Hammer, H.-P. Stunk, M. Schulz, K. Heinz, *Appl. Phys. A* **1996**, *62*, 223.
[26] H. C. Card, E. H. Rhoderick, *J. Phys. D: Appl. Phys.* **1971**, *4*, 1589.
[27] S. Suzuki, T. Yamamoto, H. Suzuki, K. Kawaguchi, K. Takahashi, Y. Yoshisato, *J. Appl. Phys.* **1997**, *81*, 6830.
[28] T. Yamamoto, S. Suzuki, K. Kawaguchi, K. Takahashi, *Jpn. J. Appl. Phys.* **1998**, *37*, 4737.